

# Purification and characterization of olive (*Olea europaea* L.) peroxidase – Evidence for the occurrence of a pectin binding peroxidase

Jorge A. Saraiva \*, Cláudia S. Nunes, Manuel A. Coimbra

*Departamento de Química, Universidade de Aveiro, Campus Universitário de Santiago, 3810-193, Aveiro, Portugal*

Received 14 February 2006; received in revised form 6 April 2006; accepted 6 April 2006

## Abstract

Peroxidase from olive fruit (*Olea europaea* L., cv Douro) in a black ripening stage was purified to electrophoretic homogeneity, resulting in four cationic and four anionic fractions. The anionic fractions accounted for 92% of recovered activity and showed molecular masses of 18–20 kDa. The anionic fraction PODa4, the predominant fraction that comprised about 70% of total recovered activity, showed an isoelectric point of 4.4 and optimum pH and temperature of, respectively, 7.0 and 34.7 °C, and apparent  $K_m$  values of 41.0 and 0.53 mM, for phenol and H<sub>2</sub>O<sub>2</sub>, respectively. From the activity-temperature profile, the denaturation temperature and the changes in enthalpy and heat capacity for unfolding of PODa4 were estimated as being, respectively, 36.5 °C, 411.2 and –13.6 kJ mol<sup>-1</sup> K<sup>-1</sup>. The activation energy for phenol oxidation by PODa4 was 99.1 kJ mol<sup>-1</sup>, corresponding to a calculated temperature coefficient ( $Q_{10}$ ) of 4. The arabinose (39 mol%) and galacturonic acid (38 mol%) content of the carbohydrate moiety indicated the existence of pectic material in the purified PODa4 fraction. Co-migration of the carbohydrate with the protein band in the isoelectric focusing electrophoresis, points to PODa4 fraction as being a pectin type binding peroxidase.

© 2006 Elsevier Ltd. All rights reserved.

**Keywords:** *Olea europaea* L.; Olive peroxidase; Enzyme purification; Pectin; Unfolding

## 1. Introduction

Peroxidases (donor: H<sub>2</sub>O<sub>2</sub> oxidoreductase, EC 1.11.1.7; POD) are glycoproteins with ubiquitous distribution in the plant kingdom, showing generally several isoenzyme forms, high thermo-resistance and activity regeneration after heat inactivation (Vámos-Vigýázó, 1981). The multiple isoperoxidase forms found within the same plant source can differ with respect to molecular mass, isoelectric point, pH and temperature optima, substrate specificity, amino acid and sugar compositions, and heat stability. Physiological functions of POD include lignification, suberisation and wound healing, general stress response, and protection against pathogen attack (Veitch, 2004). In raw and pro-

cessed foods POD activity has been associated with adverse changes of flavour, colour, texture, and nutritional value (Fils, Sauvage, & Nicolas, 1985).

Due to its high thermal stability and easiness of activity quantification, peroxidase residual activity is frequently used to determine whether the heat processing of vegetables has been adequate. Peroxidases are also becoming increasingly attractive catalysts to generate free radicals to synthesize a variety of polymers (Kobayashi, Uyama, & Kimura, 2001), to promote stereospecific biotransformation of organic molecules (Adam et al., 1999), and for bioremediation (Klibanov, Tu, & Scott, 1983).

Olive fruit is used for oil extraction and also for consumption as table olive after processing. Texture and consistency are important quality characteristics of table olives that can be influenced by the catalytic action of peroxidase, since it has been associated with cell wall stiffening (Shah,

\* Corresponding author. Tel.: +351 234370716; fax: +351 234370084.  
E-mail address: [jsaraiva@dq.ua.pt](mailto:jsaraiva@dq.ua.pt) (J.A. Saraiva).

Penel, Gagnon, & Dunand, 2004). POD activity in olive fruit appears at the turning colour stage of ripening and increases significantly in the full black ripened fruit (Garrido Fernández, Fernández Díez, & Adams, 1997), as observed also for polyphenoloxidase (Mafra et al., 2006). The Portuguese Douro cultivar is one of the few cultivars that produce fruits that can be harvested at the black ripening stage, to be processed for consumption as black oxidised table olives, resulting in a final product with good texture properties. This feature was attributed to an increase of both skin strength and stiffness caused by ripening (Georget, Smith, & Waldron, 2001), that prevents detrimental effects on texture caused by processing.

The objective of this work was to purify and characterize, for the first time, olive POD from naturally black olives, of the Portuguese Douro cultivar, to further study the possible contribution of olive POD to the peculiar texture characteristics of Douro cultivar black ripened olive. Olive POD was characterized with respect to molecular mass and isoelectric point, catalytic properties for the oxidation of phenol, and denaturation temperature. Carbohydrate content and composition of the glycosidic fraction linked to the main olive POD fraction was also studied.

## 2. Experimental

### 2.1. General experimental procedures

Phenol, 4-aminoantipyrine, polyvinylpyrrolidone (PVPP), hydrogen peroxide (30% v/v), bicinchoninic acid (BCA) and standard bovine serum albumin protein were purchased from Sigma. Column packing materials CM-Sephadex and DEAE-Sephacel were from GE Healthcare. SDS-PAGE and IEF Standards were obtained from Bio-Rad. All other chemicals were of analytical grade.

### 2.2. Plant material

The olive fruits (*Olea europaea* L., cv Douro) used in this work, were harvested at a black ripening stage and were provided by Maçarico Ltd. table olive industry. Upon arrival at the laboratory, the fruits were frozen in liquid nitrogen and stored at  $-20\text{ }^{\circ}\text{C}$  until enzyme extraction was carried out.

### 2.3. Purification procedure

Acetone powder, used as the enzyme source, was prepared based on the method described by Civello, Martínez, Chaves, and Añón (1995) for the extraction of strawberry peroxidase, as follows. Frozen olives (100 g) were first thawed at  $4\text{ }^{\circ}\text{C}$ , destoned, and homogenized for 2 min with 1 l of cold acetone ( $-20\text{ }^{\circ}\text{C}$ ) using an Ultraturrax. The homogenate was then filtered through a glass fibre filter (Whatman GF/C), and the solid residue was washed with cold acetone, until no more colour compounds were removed by the washing, to obtain as much as possible a col-

ourless filtrate. The solid material was allowed to dry at room temperature and the powder obtained was kept at  $-20\text{ }^{\circ}\text{C}$  until use. All steps of the extraction and purification procedure were carried out at  $4\text{ }^{\circ}\text{C}$ , unless otherwise indicated.

An aqueous suspension (250 ml) in 0.05 M sodium phosphate buffer, pH 7.0, was prepared with the acetone powder obtained (ca. 20 g), according to the procedure of Ingham, Parker, and Waldron (1998). The suspension was continuously stirred for 30 min and then centrifuged at 20,000g for 20 min and the supernatant was separated. The solid residue obtained was suspended again in 50 ml of the same buffer and centrifuged alike. The two resulting supernatants were combined and used as the crude enzyme extract for the purification process.

The crude enzyme extract was brought to 30% saturation by adding slowly solid ammonium sulphate with continuous stirring for 30 min. The ppt was separated by centrifugation (20,000g for 20 min) and the ammonium sulphate saturation of the supernatant was increased to 90%, which was left under stirring for 3 h. The resulting ppt was separated by centrifugation (20,000g for 20 min), dissolved in a minimum volume of 0.05 M sodium phosphate buffer, pH 7.0, desalted by gel filtration using Sephadex G-25, and lyophilized.

The lyophilized enzyme extract was dissolved in water (10 ml) and applied to a CM-Sephadex column (GE Healthcare,  $1.6 \times 20\text{ cm}$ ), previously equilibrated with 0.05 M sodium phosphate buffer, pH 7.0, at a flow rate of  $15\text{ ml h}^{-1}$ . The column was washed with 30 ml of the buffer and the retained material was eluted using a continuous linear gradient of NaCl (0–1.3 M), at the same flow rate and with the same buffer. Fractions of 2.0 ml were collected during elution, analyzed immediately for POD activity and their absorbance measured at 280 nm. Fractions showing POD activity were collected, frozen in liquid nitrogen, and stored at  $-20\text{ }^{\circ}\text{C}$ .

The fractions' pool (12 ml) with POD activity, eluted with the washing buffer from the CM-Sephadex column, were loaded in two separated runs (5 and 7 ml each), on a DEAE-Sephacel column (GE Healthcare,  $1.6 \times 20\text{ cm}$ ) previously equilibrated with 0.01 M Tris/HCl buffer, pH 7.0. Before elution with a linear gradient of NaCl (0–1.3 M) in Tris/HCl buffer (50 ml), the column was washed with 50 ml of the same buffer without NaCl, in both cases at a flow rate of  $20\text{ ml h}^{-1}$ . Fractions were collected, and analyzed in the same manner as for cation-exchange chromatography.

### 2.4. Activity and protein quantification

Peroxidase activity was measured spectrophotometrically based on the procedure of Worthington (1993). An aliquot of enzymatic extract (50  $\mu\text{l}$ ) was added to 1.45 ml substrate solution (0.1 M sodium phosphate buffer, pH 7.0, containing 83.0 mM phenol, 1.15 mM 4-aminoantipyrine and 0.95 mM  $\text{H}_2\text{O}_2$ ), previously equilibrated for 20 min at  $25\text{ }^{\circ}\text{C}$  (Worthington, 1993; Yuan & Jiang, 2003). The increase in absorbance at 510 nm was recorded, using a Shimadzu UV-160A spectrophotometer, equipped

with a constant temperature cell holder at 25 °C. The slope ( $\Delta A_{510\text{nm}} \text{ min}^{-1}$ ) of the initial linear portion of the curve relating absorbance at 510 nm (the absorbance maximum of quinol red, the coloured reaction product) versus time, was determined to calculate the activity in nkat, using the extinction coefficient ( $6.58 \text{ M}^{-1} \text{ cm}^{-1}$ ),  $\epsilon$ , at 510 nm for quinol red (Yuan & Jiang, 2003).

Total protein content was estimated according to the bicinchoninic acid (BCA) method using bovine serum albumin (BSA) as standard (Smith et al., 1985).

### 2.5. Electrophoresis

Purity and molecular mass of the different olive POD fractions were analyzed by SDS–PAGE, under reducing and non-reducing conditions (two determinations each), with a Phast System and a homogeneous polyacrylamide gel (PhastGel Homogeneous 20 from GE Healthcare). Samples were dialysed against water using SnakeSkin™ dialysis membrane (Pierce), with a cut-off of 3500 kDa, during 12 h at 4 °C (conductivity measurements were used to determine dialysis time). After dehydration under a nitrogen stream, samples were prepared using a denaturing soln (10 mM Tris/HCl, pH 8.0, 1 mM EDTA, 2.5% (w/v) SDS and 0.01% (w/v) bromophenol blue –5% (v/v)  $\beta$ -mercaptoethanol was only used under reducing conditions). Markers with molecular masses in the range of 6.5–116.5 kDa (Bio-Rad) were used to estimate the molecular mass of the different olive POD fractions. The gels were stained using the silver staining method (Moreno, Smith, & Smith, 1985).

Isoelectric focusing was performed using a Phast System (GE Healthcare) on pre-poured gels (PhastGel 3–9) with pI standards from 4.2 to 9.6 (Bio-Rad). The POD fractions were dialysed and concentrated using the same procedures as for SDS–PAGE and the gel was also stained alike.

### 2.6. Optimum pH

Optimum pH was assayed with 0.1 M citrate, phosphate, and Tris/HCl buffers, for pH values of 4.0–5.0, 6.0–8.0, and 9.0, respectively.

### 2.7. Kinetic constants for phenol and $\text{H}_2\text{O}_2$

$K_m$  for phenol was determined by varying its concentration from 5 to 150 mM at a saturating concentration of  $\text{H}_2\text{O}_2$ . Likewise,  $K_m$  for  $\text{H}_2\text{O}_2$  (from 0.08 to 4.0 mM) was calculated at a saturating phenol concentration. In both cases least-squares nonlinear regression was used to estimate  $K_m$ , by fitting the experimental data to the Michaelis–Menten equation.

### 2.8. Denaturation and optimum temperatures

Denaturation (unfolding) temperature of olive PODa4 purified fraction was determined based on the procedure

reported by Hei and Clarck (1993), from the experimentally determined activity-temperature profile, in the range of 15–60 °C, at the optimum pH and substrates saturation concentrations.

At any temperature,  $T$ , the initial enzymatic reaction rate,  $v_0(T)$ , relates to the amount of active, native enzyme ( $N$ ), by the catalytic rate constant of the enzyme,  $k_{\text{cat}}(T)$ , and the equilibrium denaturation constant,  $K_{\text{RD}} = [D]/[N]$  (being  $D$  the amount of reversibly denatured enzyme), as follows (Hei & Clarck, 1993):

$$v_0(T) = k_{\text{cat}}(T)N = \frac{k_{\text{cat}}(T)E_0}{1 + K_{\text{RD}}(T)}, \quad (1)$$

where  $E_0$  is the total amount of enzyme ( $E_0 = N + D$ ) and  $v_0$ ,  $k_{\text{cat}}$  and  $K_{\text{RD}}$  vary with temperature.

The effect of temperature on  $k_{\text{cat}}$  is described by the Arrhenius expression:

$$k_{\text{cat}}(T) = A \exp\left(-\frac{E_a}{RT}\right), \quad (2)$$

where  $A$  is the Arrhenius pre-exponential factor,  $E_a$  is the activation energy ( $\text{kJ mol}^{-1}$ ),  $R$  is the universal gas constant ( $8.314 \times 10^{-3} \text{ mol kJ}^{-1} \text{ K}^{-1}$ ), and  $T$  is the absolute temperature (K).

Temperature dependence of  $K_{\text{RD}}$  is described by (Hei & Clarck, 1993):

$$K_{\text{RD}}(T) = \exp\left\{\frac{\Delta H_m^0}{RT_m} - \frac{\Delta C_p^0}{R}(1 + \ln(T_m)) + \left(\frac{\Delta C_p^0 T_m}{RT} - \frac{\Delta H_m^0}{R}\right)\frac{1}{T} + \frac{\Delta C_p^0}{R} \ln(T)\right\}, \quad (3)$$

where  $\Delta H_m^0$ ,  $\Delta C_p^0$ , and  $T_m$  are, respectively, the change in enthalpy for thermal unfolding at  $T_m$  and 1 atm ( $H_{\text{reversible denaturated}} - H_{\text{native}}$ ), the change in heat capacity for thermal unfolding at 1 atm ( $C_{p, \text{reversible denaturated}} - C_{p, \text{native}}$ ), and the unfolding temperature (the temperature at which  $K_{\text{RD}} = 1$  and  $[D] = [N]$ ).

Curve fitting was also carried out based on the procedure described by Hei and Clarck (1993), as follows. Linear regression was used to fit the Arrhenius relation (Eq. (2)) to the lower-temperature experimental data points. Using the estimated activation energy ( $E_a$ ), the Arrhenius pre-exponential factor ( $A$ ), and Eq. (2), the value of  $k_{\text{cat}}$  can be calculated for the higher-temperature range of the activity-temperature profile (in fact the  $k_{\text{cat}}$  calculated in this way are the values expected if no denaturation would occur). Then, these values were used to compute the values of  $K_{\text{RD}}$ , using Eq. (1). The calculated reversible denaturation equilibrium constants were then used to estimate  $\Delta H_m^0$ ,  $\Delta C_p^0$ , and  $T_m$ , by Eq. (3) and least-square nonlinear regression (MATLAB software, The MathWorks, Inc., MA, USA). To fit the whole activity-temperature profile, Eqs. (2) and (3) where combined with Eq. (1) by substituting, respectively,  $k_{\text{cat}}$  and  $K_{\text{RD}}$  into Eq. (1) to yield the final model-estimated activity-temperature profile.

The optimum temperature (the temperature at which the activity is maximal) was estimated by generating the model curve, with a temperature step increment of 0.1 K, with a maximum inaccuracy of less than 0.1 K.

### 2.9. Heat stability

Aliquots (300  $\mu$ l) of the olive POD extract purified with ammonium sulphate, were incubated at 40, 50 and 60 °C at pH 7. After 5, 10 and 15 min, aliquots were withdrawn and cooled immediately in an ice/water mixture. The residual enzymatic activity was determined after 5 min cooling and after 24 h storage at 4 °C, to check for the possible occurrence of activity regeneration.

### 2.10. Carbohydrate content and sugar analysis

Hydrolysis of the carbohydrate moiety was carried out at 100 °C using 1 M sulphuric acid during 150 min. Neutral and amine sugars were analyzed as their alditol acetates by GC (Blakeney, Harris, Henry, & Stone, 1983; Harris, Blakeney, Henry, & Stone, 1988). A Hewlett–Packard-5890 GC apparatus with split injector and a FID detector was used, with a 30 m DB-1 column (J& W) with i.d. and film thickness of 0.25 mm and 0.1  $\mu$ m, respectively. The oven temperature program used was: 100 °C for 1 min, followed by a rise in temperature at a rate of 2 °C  $\text{min}^{-1}$  up to 220 °C and then 220 °C for 1 min. The injector and detector temperatures were, respectively, 220 and 250 °C. The flow rate of the carrier gas ( $\text{H}_2$ ) was set at 39.5  $\text{ml min}^{-1}$ . Uronic acids were quantified by a colorimetric method (Blumenkrantz & Asboe-Hansen, 1973) with some modifications described by Coimbra, Delgado, Waldron, and Selvendran (1996).

The FT-IR spectra of PODa4 fraction were obtained using a Golden Gate single refraction diamond ATR system in a Bruker IFS-55 spectrometer. The spectra were recorded at the absorbance mode from 4000 to 400  $\text{cm}^{-1}$  (mid infrared region) at the resolution of 8  $\text{cm}^{-1}$  (Barros et al., 2002).

For the methylation studies, the purified enzyme sample was treated with powdered NaOH and methylated with  $\text{CH}_3\text{I}$  (Ciucanu & Kerek, 1984; Isogai, Ishizu, & Nakano,

1985) as described by Coimbra et al. (1996). The partially methylated alditol acetates were analyzed and characterized by GC–MS. This analysis was performed in a HP series 2 gas chromatograph and Trio-1S VG mass-lab with scans between 400–35  $\text{m/e/s}$  with 70 eV ionization energy. The sample was injected in splitless mode, with the injector and detector operating at 210 and 220 °C, respectively, using the following temperature program: 55 °C for 0.75 min with a linear increase of 45 °C  $\text{min}^{-1}$  up to 140 °C, and standing for 1 min at this temperature, followed by a linear increase of 2.5 °C  $\text{min}^{-1}$  up to 218 °C, with further 37 min at 218 °C using an OV-1 capillary column (30 m length, 0.32 mm of internal diameter and 0.25  $\mu$ m of film thickness). The linear velocity of the carrier gas (He) was set at 40  $\text{cm s}^{-1}$  at 200 °C, with a solvent delay of 4 min.

## 3. Results and discussion

### 3.1. Peroxidase purification

The results of the purification procedure for olive POD are summarized in Table 1. Five different fractions with POD activity were found using cationic exchange chromatography. The four retained fractions were named PODc1–4, with the (c) standing for cationic and the number indicating the order of elution. The unbound fraction, eluted with the washing buffer, was further purified by anionic exchange chromatography, resulting in four fractions showing POD activity (Fig. 1). These four retained fractions were named PODa1–4, with the (a) standing for anionic and the number indicating the order of elution. The four anionic fractions were responsible for 92% of the recovered activity, with PODa4 showing a total activity of  $6.5 \times 10^3$  nkat, comprising about 70% of the recovered activity.

### 3.2. Molecular mass and isoelectric point

SDS-PAGE of each of the eight fractions revealed a single protein band either in presence or in the absence of  $\beta$ -mercaptoethanol, indicating that all fractions were homogenous and composed by a single polypeptide chain.

Table 1  
Purification of peroxidase from black ripened olive fruit

Fraction	Protein (mg)	Total activity (nkat)	Specific activity (nkat $\text{mg}^{-1}$ )	Yield (%)	Purification (-fold)
Crude extract	2700	$6.8 \times 10^4$	25	100	1.0
$(\text{NH}_4)_2\text{SO}_4$ precipitation	680	$3.8 \times 10^4$	56	56	2.2
PODc1	0.10	$1.6 \times 10^2$	$1.6 \times 10^3$	0.2	64
PODc2	0.07	$3.3 \times 10^2$	$4.7 \times 10^3$	0.5	188
PODc3	0.03	$1.3 \times 10^2$	$4.2 \times 10^3$	0.2	168
PODc4	0.04	$2.0 \times 10^2$	$4.9 \times 10^3$	0.3	196
PODa1	1.90	$1.4 \times 10^3$	$7.3 \times 10^2$	2.0	29
PODa2	0.52	$6.2 \times 10^2$	$1.2 \times 10^3$	0.9	48
PODa3	0.72	$6.8 \times 10^2$	$9.5 \times 10^2$	1.0	38
PODa4	1.90	$6.5 \times 10^3$	$3.4 \times 10^3$	9.4	136

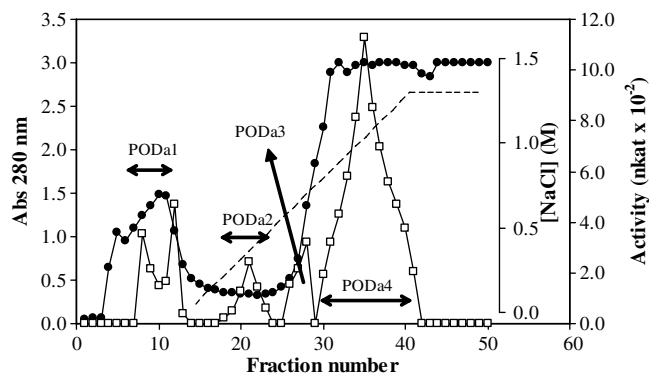


Fig. 1. DEAE-Sephacel chromatography of olive POD present in the excluded fraction from CM-Sephacel chromatography (fractions showing POD activity were named PODa1–4 according to order of elution). A NaCl linear gradient up to 1.3 M was used and 2 ml fractions were collected. Peroxidase activity (□) per 2 ml fraction, using phenol as substrate, absorbance at 280 nm (●) and, NaCl gradient (broken line).

The molecular mass of the purified fractions, determined by SDS-PAGE, under reducing and non-reducing conditions, yielded an average of 66.4, 68.6, 64.3, and 60.2 kDa, for the cationic fractions (PODc1–4, results not shown), and 18.4, 20.3, 20.1, and 20.5 kDa for the anionic fractions (PODa1–4, Fig. 2A). The molecular masses of peroxidases from several fruits and vegetables usually range from 30 to 54 kDa (Vámos-Vigýázó, 1981), but higher values have been reported by Padiglia, Cruciani, Pazzaglia, Medda, and Floris (1995) for opuntia (58 kDa) and by Civello et al. (1995) for strawberry (58 and 66 kDa) peroxidases. Although the low molecular mass for olive PODa1–4 anionic fractions found in this work is rather unusual, similar values were also reported by Khan and Robinson (1993) for two mango isoperoxidases (22 and 27 kDa). More recently, a 6 kDa peptide from *Raphanus sativus* was reported as showing peroxidase activity (Omumi, Morshedi, & Samadi, 2001). Ebrahimzadeh, Motamed, Rastgar-Jazii, Montasser-Kouhsari, and Shokraii (2003) reported that POD activity in olive increased gradually during fruit development, reaching a maximum at full fruit development and remained then constant during ripening and softening stages. Concomitantly with this pattern of activity increment, the same authors verified the appearance and increment of protein bands at 18–22 kDa, thus pointing to the occurrence of POD isoenzymes with molecular masses in this range in olive.

The four olive PODa1–4 fractions (that accounted for 92% of the recovered activity) were isoelectrically focused in a polyacrylamide gel, and appeared as a single band (Fig. 2B). The isoelectric points obtained were 6.9 for PODa1 and PODa2 and 4.6 and 4.4 for, respectively, PODa3 and PODa4. The double peak for PODa1 shown in Fig. 1 that was obtained for the two runs of the DEAE-Sephacel chromatography indicates the possible occurrence of two anionic peroxidases. However, since only one band was obtained for PODa1 with SDS-PAGE and isoelectric focusing electrophoreses, PODa1 was con-

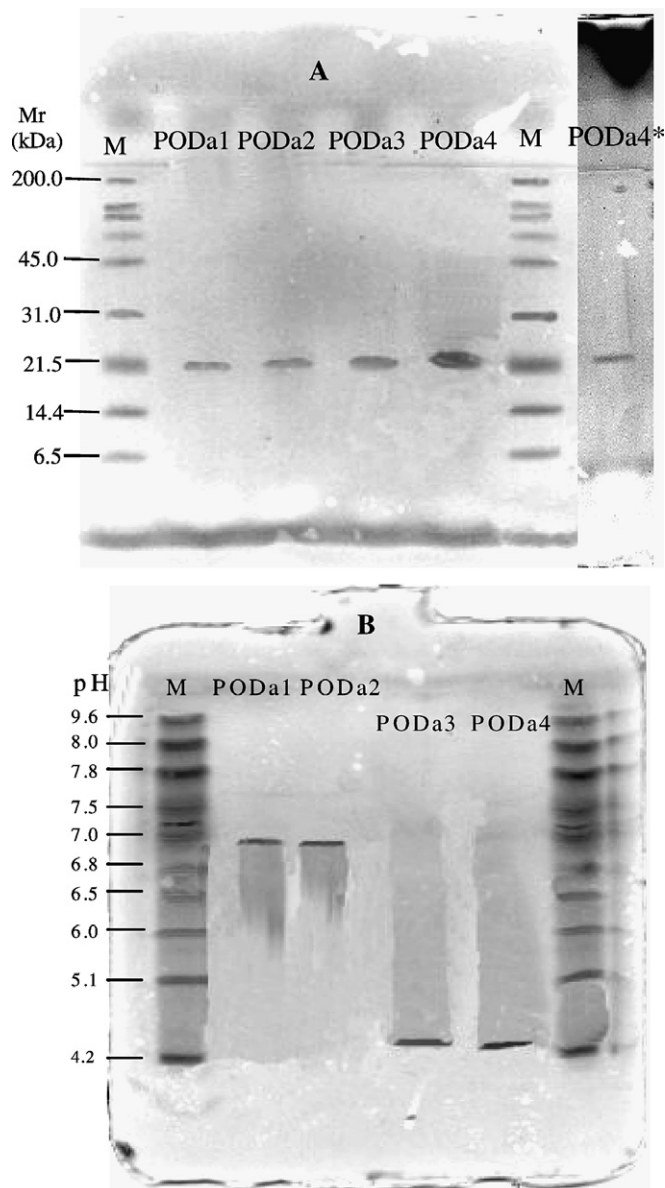


Fig. 2. (A) SDS-polyacrylamide gel electrophoresis under non-reducing conditions and (B) isoelectric focusing of olive POD purified anionic fractions (PODa1, PODa2, PODa3, and PODa4) (M stands for markers with known molecular mass or isoelectric point values, in (A) or (B), respectively). PODa4\* refers to PODa4 fraction with one fourth of the protein content used in the gel, compared to lane PODa4.

sidered as only one anionic peroxidase. Since PODa4 comprised about 70% of the total recovered activity, this fraction was further characterized for its catalytic properties for the oxidation of phenol, for its denaturation temperature, and for the quantitative identification and characterization of its glycan moiety.

### 3.3. Optimum pH

The activity of PODa4 showed a maximum at pH 7.0 and decreased steeply for higher and lower values of pH, reaching 50% of maximum activity at pH values of about

6.2 and 7.5. For comparison, it can be stated that the optimum pH for activity of horseradish peroxidase, using phenol as substrate, is also 7.0 (Worthington, 1993; Yuan & Jiang, 2003).

### 3.4. Kinetic constants for phenol and H<sub>2</sub>O<sub>2</sub>

PODa4 revealed Michaelis–Menten kinetics with both phenol and H<sub>2</sub>O<sub>2</sub>, up to a concentration of, respectively, 150 and 4.0 mM (Fig. 3). Apparent  $K_m$  values estimated using least-squares nonlinear regression were 41.0 ( $r^2 = 0.99$ ) and 0.53 mM ( $r^2 = 0.99$ ) for phenol and H<sub>2</sub>O<sub>2</sub>, respectively. The value obtained for hydrogen peroxide was very close to that obtained by Dong (2002) for horseradish peroxidase (0.43 mM), using phenol as hydrogen donor, and comparable to those reported for anionic peroxidases from melon (Rodríguez-López et al., 2000) and from turnip roots (Agostini, Medina, Milrad de Forchetti, & Tigier, 1997; Duarte-Vázquez, García-Almendárez,

Regalado, & Whitaker, 2000), with other hydrogen donors. For horseradish peroxidase, a  $K_m$  value of 13 mM for phenol was reported (Liu, Song, Weng, & Ji, 2002), which is considerably lower than the result obtained for PODa4.

### 3.5. Denaturation and optimum temperatures

Using the Arrhenius equation, a value of 99.1 kJ mol<sup>-1</sup> (Table 2) was obtained for the activation energy ( $E_a$ ) for phenol oxidation. A value of 4 was obtained for the temperature coefficient ( $Q_{10}$  – the quotient between the activity at a temperature ( $T + 10$ ) K and the activity at  $T$  K). This means that PODa4 activity doubles for each 5 °C increase. For most enzymes in homoiothermic species (e.g. mammals) the value of  $Q_{10}$  is approximately 2 (Price & Stevens, 1996). However, enzymes of poikilothermic organisms, as for example, species that have to adapt to cold conditions, usually have  $Q_{10}$  values lower than 2. Organisms with enzymes with  $Q_{10}$  values higher than 2, might experience considerable increase/decrease in metabolic reactions, when temperature increases/decreases.

The thermodynamic parameters for the reversible unfolding of PODa4 are also shown in Table 2. The value obtained for  $\Delta H_m^0$  is within the range obtained for many other proteins, while several proteins were also reported to show negative values for  $\Delta C_p^0$  for thermal unfolding (Pfeil, 1998). The value obtained for the unfolding temperature,  $T_m$ , was 36.5 °C and the temperature for maximum activity,  $T_{opt}$ , was 34.7 °C. Fig. 4 shows the experimental points and the model fitted curve, in the whole activity-temperature range.

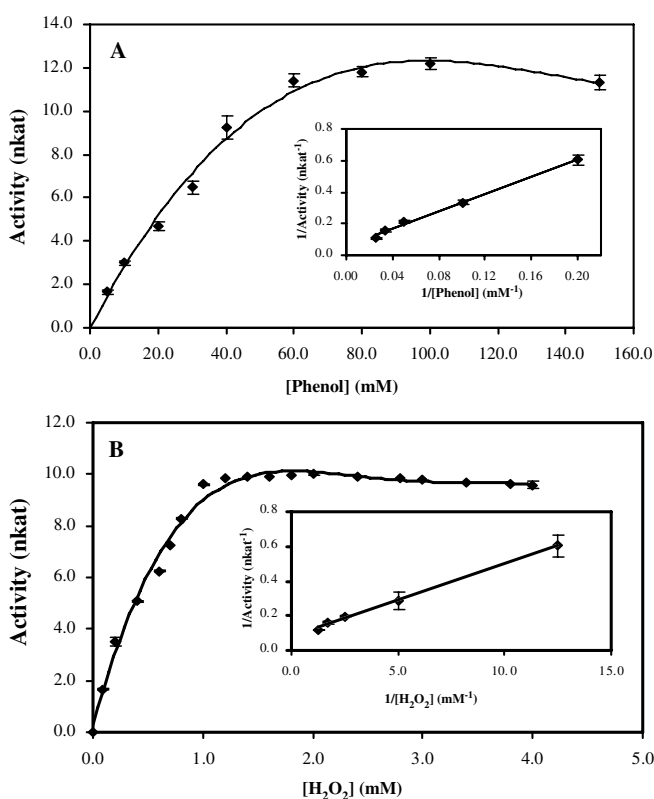


Fig. 3. Effect of (A) phenol and (B) hydrogen peroxide concentration on activity of olive peroxidase anionic fraction PODa4 (insets: Lineweaver–Burk plots). Vertical bars represent  $\pm$ SD (three determinations).

Table 2

Parameters obtained from the Arrhenius fit ( $E_a$  and  $A$ ), for the fit of the thermal denaturation (Eq. (3),  $\Delta H_m^0$ ,  $\Delta C_p^0$ , and  $T_m$ ), respectively, for the low- and high-temperature ranges of the activity-temperature profile of phenol oxidation by PODa4, and for the estimation of  $T_{opt}$  (errors indicated are  $\pm$  95% confidence interval)

$E_a$ (kJ mol <sup>-1</sup> )	$A$	$\Delta H_m^0$ (kJ mol <sup>-1</sup> )	$\Delta C_p^0$ (kJ mol <sup>-1</sup> K <sup>-1</sup> )	$T_m$ , K (°C)	$T_{opt}$ , K (°C)
99.1 $\pm$ 16.4	1.54 $\times$ 10 <sup>19</sup> ( $r^2 = 0.97$ )	4 11.2 $\pm$ 62.2	-13.6 $\pm$ 4.5	309.7 $\pm$ 0.5 (36.5)	307.9 $\pm$ <0.1 (34.7)

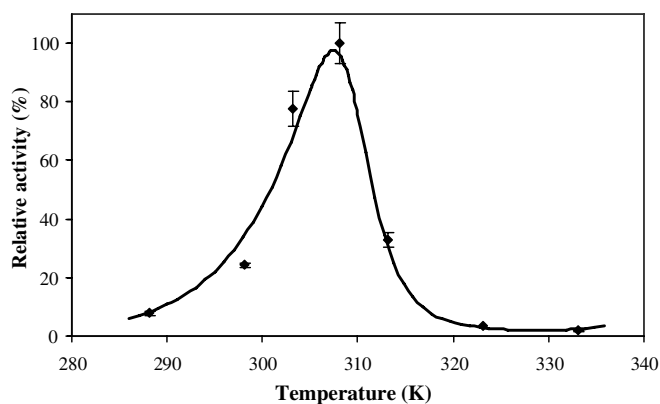


Fig. 4. Activity-temperature profile obtained for the oxidation of phenol by PODa4. The model curve was obtained by fitting the experimental data to the equation obtained by combining Eqs. (1)–(3). Vertical bars represent  $\pm$ SD (at least two determinations).

### 3.6. Thermal stability

An exploratory study of the thermal stability of olive POD was undertaken using the extract obtained after ammonium sulphate fractionation and desalting, which is representative of all eight POD fractions found in olive fruit. Heating at 40 °C for 5 and 10 min, caused 60% and 85% reduction of activity, respectively, and no measurable activity could be detected upon heating at 50 and 60 °C for 5 min, indicating a moderate thermal stability that is in accordance with the relatively low value obtained for  $T_m$  of PODa4. The enzyme was not able to regain activity upon inactivation and storage at 4 °C for 24 h.

### 3.7. Carbohydrate content and glycosidic-linkage analysis

The glycosidic fraction of PODa4 was constituted mainly by arabinose (39 mol%) and uronic acids (38%). Glucose (10%), rhamnose (6%), galactose (4%), fucose (1%), xylose (1%) and mannose (1%) were also detected, but in minor quantities. Similar results were found for PODa3 fraction. Chemical deglycosylation using TFA 1.0 M, 3 h, 120 °C, instead of sulphuric acid, yielded identical values for both PODa3 and PODa4 fractions (results not shown). With both deglycosylation procedures neither glucosamine nor galactosamine were detected. Although the sugar composition of the glycosidic part of PODa1 and PODa2 fractions was not determined, the presence of uronic acids in these fractions by the *m*-phenylphenol colorimetric assay was verified (Blumenkrantz & Asboe-Hansen, 1973; Coimbra et al., 1996). The presence of galactose, fucose, xylose, and mannose, and the relative amounts of the latter three sugars, points to PODa3 and PODa4 having a glycan moiety characteristic for the “complex type” of glycoproteins (Dwek, 1996; Freeze, 2000), as was reported for petunia (Hendriks & van Loon, 1990), horseradish (Kurosaka et al., 1991), and peanut (Shaw, Sun, Barber, & van Huystee, 2000; Sun, Lige, & van Huystee, 1997) peroxidases. Arabinose and glucose were also reported to be present in petunia (Hendriks & van Loon, 1990), horseradish (Clark & Shannon, 1976), and tobacco (Choy, Wong, Lau, & Yung, 1979) peroxidases. The origin of these sugars (and of rhamnose and uronic acids) may be related to the presence of cell wall pectic polysaccharides, as was proposed for petunia peroxidase (Hendriks & van Loon, 1990).

To evaluate such a possibility, a FT-IR analysis was carried out for the purified PODa4. The pectic polysaccharides characteristic bands at 1150, 1100 and 1020  $\text{cm}^{-1}$  (Coimbra, Barros, Barros, Rutledge, & Delgado, 1998) present in the FT-IR spectrum clearly indicated the presence of pectic polysaccharides. The presence of pectic polysaccharides was also observed by methylation analysis of the arabinan moiety, which allows to determine the type of glycosidic linkages present. The results (not shown) revealed an arabinosyl composition that although more branched, is characteristic of the arabinan that occurs as side chains of olive pulp pectic polysaccharides (Cardoso, Silva, & Coimbra, 2002).

To eliminate the possibility of the presence of these pectic polysaccharides as an artefact of the purification procedure, namely, to discard the possible presence of polysaccharides in the gels obtained by isoelectric focusing electrophoresis, the phenol–sulphuric acid method (Dubois, Gilles, Hamilton, Rebers, & Smith, 1956) that allows the detection of sugars was applied. The results indicated the presence of polysaccharides only at the positions coincident with the four olive POD anionic protein bands, as seen by the appearance of a brown colour. These results point to the presence of pectic polysaccharides, in olive PODa1–4 purified fractions, possibly linked to the enzyme, since it is not expected that the pectic polysaccharides, due to their heterogeneity, would behave the same way as the enzyme during ammonium sulphate fractionation, ionic chromatographies, and isoelectric focusing electrophoresis.

Some peroxidase isoenzymes from lupin (Ros Barceló, Pedreño, Muñoz, & Sabater, 1988), zucchini (Penel & Greppin, 1994; Penel & Greppin, 1996) horseradish (Penel, Crèvecoeur, & Greppin, 1996), and *Arabidopsis* leaves (Shah et al., 2004), have been reported to show a specific binding affinity for low methylesterified pectins in the presence of calcium. These peroxidases bind specifically to the homogalacturonan domains of pectin chains, in their  $\text{Ca}^{2+}$ -pectate conformation, a structure called ‘egg-box’ or junction zone (Carpita & Gibeaut, 1993; Jarvis, 1984). The  $\text{Ca}^{2+}$ -pectate affinity exhibited by these peroxidases was proposed to possibly function as a spatial distribution control mechanism within the cell wall matrix (Carpin et al., 2001), since the  $\text{Ca}^{2+}$ -pectate conformation of pectins occurs mainly in middle lamella and cell corners (McCann & Roberts, 1996). The interaction between zucchini peroxidase and pectin was found to be of electrostatic nature, although resisting relatively high concentrations of NaCl (Carpin et al., 2001).

The results obtained in this work for fractions PODa1–4 support the hypothesis that olive peroxidase is a peroxidase that binds specifically to pectic polysaccharides, with a very low molecular mass and very low degree of methyl esterification. Ripening of olive fruit was found to cause significant depolymerization of olive fruit cell wall pectic polysaccharides (Mafra et al., 2006, 2001), with the consequent formation of a relative higher proportion of lower molecular mass pectic material. In addition, the degree of methyl esterification of olive pectic polysaccharides decreases from 71% to 35%, from green to black olives (Mafra et al., 2001). In this way, low methylesterified and low molecular mass pectic material is present in black ripened olives that can bind to olive POD.

### Acknowledgements

The authors acknowledge the financial support from Universidade de Aveiro (UA), Fundação para a Ciência e Tecnologia (Grant SFRH/BM/2399/2000), European Union (OLITEXT project, FAIR CT97-3053), and Dr. Theo Hendriks, from Wageningen University & Research Centre,

Netherlands and Dr. Carlos Regalado from Universidad Autónoma de Querétaro, Mexico, for helpful discussions concerning the glycosidic moiety of olive peroxidase.

## References

- Adam, W., Lazarus, M., Saha-Moller, C. R., Weichold, O., Hoch, U., Haring, D., et al. (1999). Biotransformations with peroxidases. *Advances in Biochemical Engineering/Biotechnology*, 63, 73–108.
- Agostini, E., Medina, M. I., Milrad de Forchetti, S. R., & Tigier, H. (1997). Properties of two anionic peroxidase isoenzymes from turnip (*Brassica napus* L.) roots. *Journal of Agricultural and Food Chemistry*, 45, 596–598.
- Barros, A. S., Mafra, I., Ferreira, D., Cardoso, S., Reis, A., Lopes da Silva, J. A., et al. (2002). Determination of the degree of methylesterification of pectic polysaccharides by FT-IR using an Outer Product PLS1 regression. *Carbohydrate Polymers*, 50, 85–94.
- Blakeney, A. B., Harris, P. J., Henry, R. J., & Stone, B. A. (1983). A simple and rapid preparation of alditol acetates for monosaccharide analysis. *Carbohydrate Research*, 113, 291–299.
- Blumenkrantz, N., & Asboe-Hansen, G. (1973). New method for quantitative determination of uronic acids. *Analytical Biochemistry*, 54, 484–489.
- Cardoso, S. M., Silva, A. M. S., & Coimbra, M. A. (2002). Structural characterisation of the olive pomace pectic polysaccharide arabinan side chains. *Carbohydrate Research*, 337, 917–924.
- Carpin, S., Crèvecoeur, M., de Meyer, M., Simon, P., Greppin, H., & Penel, C. (2001). Identification of a Ca<sup>2+</sup>-pectate binding site on an apoplastic peroxidase. *Plant Cell*, 13, 511–520.
- Carpita, N. C., & Gibeau, D. M. (1993). Structural models of primary-cell walls in flowering plants – consistency of molecular-structure with the physical properties of the walls during growth. *The Plant Journal*, 3, 1–30.
- Choy, Y. M., Wong, Y. S., Lau, K. M., & Yung, K. H. (1979). Thermal activation of peroxidase from tobacco leaf mesophyll cell walls. *International Journal of Peptide and Protein Research*, 14, 1–4.
- Ciucanu, I., & Kerek, F. (1984). A simple and rapid method for permethylation of carbohydrates. *Carbohydrate Research*, 131, 209–217.
- Civello, P. M., Martínez, G. A., Chaves, A. R., & Añón, M. C. (1995). Peroxidase from strawberry fruit (*Fragaria ananassa* Duch.): partial purification and determination of some properties. *Journal of Agricultural and Food Chemistry*, 43, 2596–2601.
- Clark, J., & Shannon, L. M. (1976). The isolation and characterisation of the glycopeptides from horseradish peroxidase isoenzyme C. *Biochimica et Biophysica Acta*, 427, 428–442.
- Coimbra, M. A., Barros, A., Barros, M., Rutledge, D. N., & Delgadillo, I. (1998). Multivariate analysis of uronic acid and neutral sugars in whole pectic samples by FT-IR spectroscopy. *Carbohydrate Polymers*, 37, 241–248.
- Coimbra, M. A., Delgadillo, I., Waldron, K. W., & Selvendran, R. R. (1996). Isolation and analysis of cell polymers from olive pulp. In H. F. Linskens & J. F. Jackson (Eds.), *Modern methods of plant analysis* (Vol. 17, pp. 18–44). Berlin: Springer.
- Dong, H. (2002). Organic–inorganic hybrid mesoporous materials and their application as host matrix for protein molecules. PhD thesis (pp. 136–137), Drexel University, Philadelphia.
- Duarte-Vázquez, M. A., García-Almendárez, B., Regalado, C., & Whitaker, J. R. (2000). Purification and partial characterization of three turnip (*Brassica napus* L. Var. esculenta D.C.) peroxidases. *Journal of Agricultural and Food Chemistry*, 48, 1574–1579.
- Dubois, M., Gilles, K. A., Hamilton, J. K., Rebers, P. A., & Smith, F. (1956). Colorimetric method for determination of sugars and related substances. *Analytical Chemistry*, 28, 350–356.
- Dwek, R. A. (1996). Glycobiology: toward understanding the function of sugars. *Chemical Reviews*, 96, 683–720.
- Ebrahimzadeh, H., Motamed, N., Rastgar-Jazii, F., Montasser-Kouhsari, S., & Shokraii, E. H. (2003). Oxidative enzyme activities and soluble protein content in leaves and fruits of olives during ripening. *Journal of Food Biochemistry*, 27, 181–196.
- Fils, B., Sauvage, F. X., & Nicolas, J. (1985). Tomato peroxidase purification and some properties. *Sciences des Aliments*, 5, 217–232.
- Freeze, H. H. (2000). Endoglycosidase and glycoamidase release of N-linked oligosaccharides. In J. E. Colligan, B. M. Dunn, H. N. Ploegh, D. W. Speicher, & P. T. Wingfield (Eds.), *Current protocols in protein science* (Vol. 2, pp. 12.4.1–12.4.6). New York: Wiley.
- Garrido Fernández, A., Fernández Díez, M. J., & Adams, M. R. (1997). Physical and chemical characteristics of the olive fruit. In A. G. Fernández, M. J. F. Díez, & M. R. Adams (Eds.), *Table olives – production and processing* (pp. 66–109). London: Chapman & Hall.
- Georget, D. M. R., Smith, A. C., & Waldron, K. W. (2001). Effect of ripening on the mechanical properties of Portuguese and Spanish varieties of olive (*Olea europaea* L.). *Journal of Agricultural and Food Chemistry*, 81, 448–454.
- Harris, P. J., Blakeney, A. B., Henry, R. J., & Stone, B. A. (1988). Gas chromatographic determination of the monosaccharide composition of plant cell wall preparations. *Journal of the Association of Official Analytical Chemists*, 71, 272–275.
- Hei, D. J., & Clarck, D. S. (1993). Estimation of melting curves from enzymatic activity-temperature profiles. *Biotechnology and Bioengineering*, 42, 1245–1251.
- Hendriks, T., & van Loon, L. C. (1990). The nature of the heterogeneity of petunia peroxidase a. *Journal of Plant Physiology*, 136, 526–531.
- Ingham, L. M., Parker, M. L., & Waldron, K. W. (1998). Peroxidase: changes in soluble and bound forms during maturation and ripening of apples. *Physiologia Plantarum*, 102, 93–100.
- Isogai, A., Ishizu, A., & Nakano, J. (1985). A new facile methylation method for cell-wall polysaccharides. *Carbohydrate Research*, 138, 99–108.
- Jarvis, M. C. (1984). Structure and properties of pectin gels in plant-cell walls. *Plant Cell and Environment*, 7, 153–164.
- Khan, A. A., & Robinson, D. S. (1993). Purification of an anionic peroxidase isoenzyme from mango (*Mangifera indica* L. var. *Chausa*). *Food Chemistry*, 46, 61–64.
- Klibanov, A. M., Tu, T. M., & Scott, K. P. (1983). Peroxidase-catalysed removal of phenols from coal-conversion waste waters. *Science*, 221, 259–261.
- Kobayashi, S., Uyama, H., & Kimura, S. (2001). Enzymatic polymerization. *Chemical Reviews*, 101, 3793–3818.
- Kurosaka, A., Yano, A., Itoh, N., Kuroda, Y., Nakagawa, T., & Kawasaki, T. (1991). The structure of a neural specific carbohydrate epitope of horseradish-peroxidase recognized by anti-horseradish peroxidase antiserum. *The Journal of Biological Chemistry*, 266, 4168–4172.
- Liu, J. Z., Song, H. Y., Weng, L. P., & Ji, L. N. (2002). Increased thermostability and phenol removal efficiency by chemical modified horseradish peroxidase. *Journal of Molecular Catalysis B: Enzymatic*, 18, 225–232.
- Mafra, I., Barros, A. S., Nunes, C., Vitorino, R., Saraiva, J., Smith, A., et al. (2006). Ripening-related changes in the cell walls of olive (*Olea europaea* L.) pulp of two consecutive harvests. *Journal of the Science of Food and Agriculture*, 86, 988–998.
- Mafra, I., Lanza, B., Reis, A., Marsilio, V., Campestre, C., De Angelis, M., et al. (2001). Effect of ripening on texture, microstructure and cell wall polysaccharide composition of olive fruit (*Olea europaea*). *Physiologia Plantarum*, 111, 439–447.
- McCann, M., & Roberts, K. (1996). Plant cell wall architecture: The role of pectins. In J. Visser & A. G. J. Voragen (Eds.), *Pectins and pectinases* (pp. 91–107). Amsterdam: Elsevier.
- Moreno, M. R., Smith, J. F., & Smith, R. V. (1985). Silver Staining of proteins in polyacrylamide gels: increased sensitivity through a combined coomassie blue-silver staining procedure. *Analytical Biochemistry*, 151, 466–470.



- Omumi, A., Morshedi, D., & Samadi, A. (2001). Isolation of a novel stable peptide from cultivated *Raphanus sativus* with peroxidase activity. *World Journal of Microbiology and Biotechnology*, *17*, 827–828.
- Padiglia, A., Cruciani, E., Pazzaglia, G., Medda, R., & Floris, G. (1995). Purification and characterization of opuntia peroxidase. *Phytochemistry*, *38*, 295–297.
- Penel, C., & Greppin, H. (1994). Binding of plant isoperoxidases to pectin in the presence of calcium. *FEBS Letters*, *343*, 51–55.
- Penel, C., & Greppin, H. (1996). Pectin binding proteins: characterization of the binding and comparison with heparin. *Plant Physiology and Biochemistry*, *34*, 479–488.
- Penel, C., Crèvecoeur, M., & Greppin, H. (1996). The binding of peroxidases to pectins. In C. Obinger, U. Burner, R. Ebermann, C. Penel, & H. Greppin (Eds.), *Plant peroxidases: Biochemistry and physiology* (pp. 259–263). Geneva: University of Geneva Press.
- Pfeil, W. (1998). Protein stability and folding. *A collection of thermodynamic data*. Berlin: Springer.
- Price, C. N., & Stevens, L. (1996). An introduction to enzyme kinetics. *Fundamentals of enzymology*. Oxford: Oxford University Press (pp. 158–160).
- Rodríguez-López, J. N., Espín, J. C., Amor, F., Tudela, J., Martínez, V., Cerdá, A., et al. (2000). Purification and kinetic measurement of an anionic peroxidase from melon (*Cucumis melo* L.) cultivated under different salinity conditions. *Journal of Agricultural and Food Chemistry*, *48*, 1537–1541.
- Ros Barceló, A., Pedreño, M. A., Muñoz, R., & Sabater, F. (1988). Lupin peroxidases. II. Binding of acidic isoperoxidases to cell walls. *Physiologia Plantarum*, *73*, 238–244.
- Shah, K., Penel, C., Gagnon, J., & Dunand, C. (2004). Purification and identification of a  $\text{Ca}^{2+}$ -pectate binding peroxidase from *Arabidopsis* leaves. *Phytochemistry*, *65*, 307–312.
- Shaw, G. S., Sun, Y., Barber, K. R., & van Huystee, R. B. (2000). Sequence specific analysis of the heterogeneous glycan chain from peanut peroxidase by H-1-NMR spectroscopy. *Phytochemistry*, *53*, 135–144.
- Smith, P. K., Krohn, R. I., Hermanson, G. T., Mallia, A. K., Gartner, F. H., Provenzano, M. D., et al. (1985). Measurement of protein using bicinchoninic acid. *Analytical Biochemistry*, *150*, 76–85.
- Sun, Y., Lige, B., & van Huystee, R. B. (1997). HPLC Determination of the sugar compositions of the glycans on the cationic peanut peroxidase. *Journal of Agricultural and Food Chemistry*, *45*, 4196–4200.
- Vámos-Vig'yázó, L. (1981). Polyphenol oxidase and peroxidase in fruits and vegetables. *Critical Reviews in Food Science and Nutrition*, *15*, 49–127.
- Veitch, N. C. (2004). Horseradish peroxidase: a modern view of a classic enzyme. *Phytochemistry*, *65*, 249–259.
- Worthington Biochemical Corporation (1993). *Worthington enzyme manual. Enzymes and related biochemicals*. Bedford: Millipore Corporation, pp. 293–294.
- Yuan, Z. Y., & Jiang, T. J. (2003). Horseradish peoxidase. In J. R. Whitaker, A. G. J. Voragen, & D. W. S. Wong (Eds.), *Handbook of food enzymology* (pp. 408). Basel: Marcel Dekker Inc.